PETROLEUM EXPLORATION AND DEVELOPMENT
Volume 47, Issue 4, August 2020
Online English edition of the Chinese language journal

Available online at www.sciencedirect.com
ScienceDirect

Cite this article as: PETROL. EXPLOR. DEVELOP., 2020, 47(4): 762–772.

RESEARCH PAPER

Sedimentary and reservoir architectures of MB1-2 sub-member of Middle Cretaceous Mishrif Formation of Halfaya Oilfield in Iraq

SUN Wenju[1, 2], QIAO Zhanfeng[3, 4,*], SHAO Guanming[3, 4], SUN Xiaowei[3, 4], GAO Jixian[2], CAO Peng[3, 4], ZHANG Jie[3, 4], CHEN Wangang[2]

1. PetroChina Research Institute of Petroleum Exploration & Development, Beijing 100083, China;
2. China United Coalbed Methane Corp., Ltd., Beijing 100011, China;
3. PetroChina Hangzhou Research Institute of Geology, Hangzhou 310023, China;
4. CNPC Key Laboratory of Carbonate Reservoir, Hangzhou 310023, China

Abstract: Based on comprehensive analysis of core, cast thin section, logging and seismic data, the sedimentary and reservoir architectures of the MB1-2 sub-member of Mishrif Formation in Halfaya Oilfield, Iraq, are studied. The MB1-2 sub-member of Mishrif Formation has three types of microfacies, lagoon, bioclastic shoal, and tidal channel, and facies architecture controlled by sequence stratigraphy. In the 4th-order sequence, the lagoon facies aggradated vertically, and the bioclastic shoals in lenticular shape embed in the background of lagoon, the end of the sequence is incised by the "meandering river" shape tide channel, which represents the depositional discontinuity. Three types of reservoirs including tidal channel grainstone to packstone reservoirs, bioclastic shoal grainstone to packstone reservoirs and dissolved lagoon wackestone reservoirs are developed. The reservoir architectures within tidal channel and bioclastic shoal are strickly controlled by grainy facies, whereas the dissolved lagoon reservoirs controlled by both facies and dissolution are related to the sequence boundary. The reservoir sections occur mainly in the 4th sequence highstand systems tract (HST) and are separated by barriers formed in the transgressive systems tract (TST). Complicated facies architecture and dissolution modification resulted in strong heterogeneity within the reservoir, which showed the characteristics of "attic type" architecture. The results of this study can guide the development of similar reservoirs in the Middle East.

Key words: Iraq; Halfaya Oilfield; Cretaceous; Mishrif Formation; sedimentary microfacies; reservoir architecture

Introduction

The Cretaceous Mishrif Formation is a key reservoir and pay in the Middle East[1–5]. The development of the Halfaya, Sigur, Majilon and other oilfields in southern Iraq shows that the main production capacity of the Middle Cretaceous Mishrif Formation comes from the high-energy coarse-grained bioclastic grainstones in the lower section of the Formation[6–10]. The reservoir pores are mainly intergranular (dissolved) pores and intragranular (dissolved) pores. The types, features and development characteristics of the pores are similar to those of clastic rocks. The reservoirs have been studied in depth and have achieved good development effect[11–13]. However, with the development of the oilfield going on, the reservoirs have a limited production potential and cannot meet the needs anymore, and there is an urgent need to find replacement areas.

Besides the high-energy coarse-grained bioclastic limestone in the lower member of Mishrif Formation, the MB1-2 sub-member of the upper member of the Mishrif Formation has a large set of relatively low-energy fine-grained carbonate rocks (mainly packstone or wackestone), which is characterized by relatively weak rock structure differentiation, large thickness, wide distribution area and high contribution ratio of reserves[14–15]. The reservoirs contribute more than 59.74% of the reserves in the Halfaya Oilfield, and have a great potential in oil and gas development. With the increase of wells drilled, problems such as low reservoir drilling rate and unknown regularity of water injection effect come out gradually, revealing strong heterogeneity of these reservoirs. Zhong et al.[16] and Zhao Limin et al.[13] pointed out that this type of reservoir was mainly controlled by sedimentary microfacies and karstification in early karst diagenesis. Zhong et al.[17]

Received date: 13 Oct. 2019; **Revised date:** 01 Apr. 2020.
*** Corresponding author.** E-mail: qiaozf_hz@petrochina.com.cn
Foundation item: Supported by the China National Science and Technology Major Project (2016ZX05004-002).
https://doi.org/10.1016/S1876-3804(20)60091-X

have made deep analysis on the rock microfacies of Mishrif Formation, however, the current understandings on sedimentary microfacies and reservoir architectures are not deep enough, hindering well location optimization, well type optimization, water injection design, and reservoir development effect.

The study on sedimentary and reservoir architectures started from clastic rock. Miall[18] defined the classification scheme of fluvial sediment architectures with 8-level boundaries, 20 lithofacies types and 9 structural units, which has been widely applied in clastic rock reservoirs[19–21]. Due to strong epigenetic reformation, carbonate rocks often have inconsistent sedimentary and reservoir architectures, so the study on sedimentary and reservoir architectures of carbonate rock is more difficult and is still in the initial stage. Sedimentary and reservoir architectures of carbonate oolitic shoal were studied preliminarily by outcrop geological modeling[22–24], but to date, the research on underground deposition and reservoir architecture of carbonate rock is still insufficient.

Abundant data of MB1-2 sub-member of the Mishrif Formation in the Halfaya Oilfield has been collected, including 6 cored wells (1 well was cored in the whole section), logging data of more than 260 wells, and high-quality 3D seismic data, which lay a sound basis for studying 3D sedimentary and reservoir architectures. In this study, by comprehensive analysis of core, logging, seismic and other data, the sedimentary architectures were described in detail, and reservoir architectures were worked out to provide constructive suggestions for the optimization of reservoir development strategy. The study results will provide important guidance for the future development of similar reservoirs in the Middle East.

1. Geological background

The Halfaya Oilfield is located in Missan Province, Southeast of Iraq[25–26]. Located in the fore deep zone of Mesopotamia basin tectonically, it is a northwest-southeast direction wide and gentle long axis anticline (Fig. 1a). It is formed in the Neogene Zagros orogeny[27–29]. The Middle Cretaceous Mishrif Formation is the main production layer of the oilfield.

The Middle–Lower Cretaceous Sanoman-Tulonian cycle in the Middle East start with the marl of Ahmadi Formation in transgressive period, followed by the shelf Cretaceous sediments of Rumaila Formation, and then the carbonate sediments of Mishrif Formation in regression period. The top surface of the cycle is the regional unconformity of the Middle Cretaceous top, which is covered by the open platform carbonate rocks of Upper Cretaceous Khasib Formation and Tanuma Formation[30–31]. The Mishrif Formation was deposited in the Late Middle Cretaceous. The platform shoal facies of Halfaya Oilfield is a belt striking in southeast direction at the border of Iran and Iraq, and to the Basra area. It is connected with the Arabian shield in the South, and is about 350–400 m thick. It is adjacent to the sub-basin deepwater facies in the southwest, and gradually thins to 150 m. To the northwest in Iran was the Tethys Ocean in the depositional stage of Mishrif Formation[32–33].

The Mishrif Formation is further subdivided into four members, MA, MB1, MB2 and MC, and 15 sub-members (Fig. 1b), constituting five third-level sequences. The top surface of

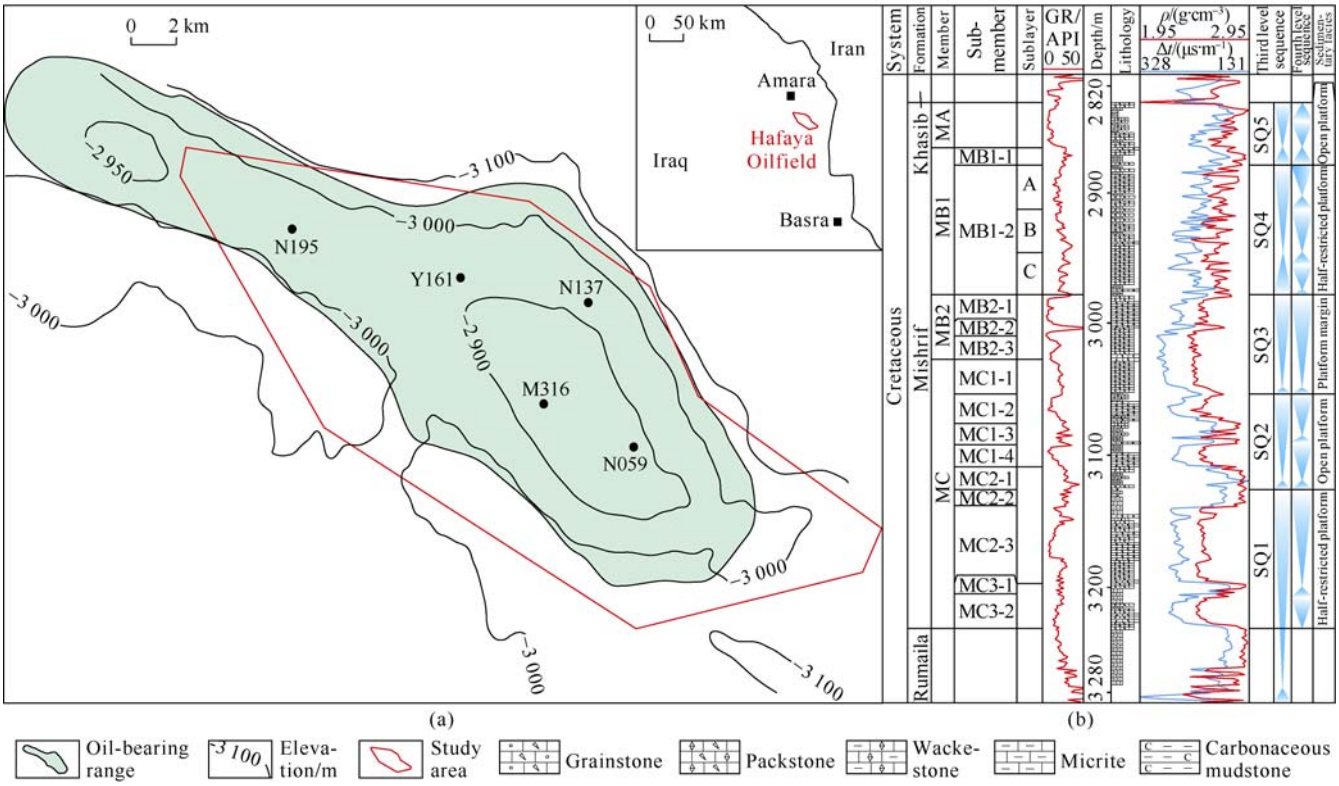

Fig. 1. Structural and well location map (a) and composite columnar section of Mishrif Formation (b) in Halfaya Oilfield, Iraq. GR—natural gamma, ρ—denstiy; Δt—acoustic differential time.

each third-level sequence is defined by typical facies such as tidal channel, incised valley or unconformity surface which represents significant sea-level fall (Fig. 1b). The main production layers of the Mishrif Formation are MB2 Member and MB1 Member. MB2 Member is mainly coarse-grained bioclastic limestone about 30 m thick, with good physical properties and high oil production[12]. The MB1 Member about 100 m thick is sub-divided into MB1-1sub-member and MB1-2 sub-member. The MB1-1 sub-member about 10–20 m thick is mainly composed of tight micrite limestone, and has hardly any reservoir. The MB1-2 sub-member is sub-divided into MB1-2A, MB1-2B and MB1-2C3 sub-layer, and is composed of fine-grained carbonate rock dominated by packstone and wackestone (Fig. 1b), mixed with a small amount of coarse-grained bioclastic limestone. With large reserves and strong heterogeneity, it is the focus of this study.

2. Sedimentary architectures

According to the sedimentary characteristics of MB1-2 sub-member of Mishrif Formation, the sedimentary architectures were studied in two levels: microfacies and coupling of microfacies architectures.

2.1. Types and architectures of sedimentary microfacies

Constrained by regional geological background, based on analysis of cores from 5 wells and 402 thin sections, combined with logging and seismic response characteristics, architectures of three microfacies identified in MB1-2 sub-member, lagoon, bioclastic shoal and tidal channel, were studied.

2.1.1. Lagoon microfacies

2.1.1.1. Composition of lagoon microfacies

This microfacies is dominated by wackestone, mixed with thin layers of micrite limestone and a small amount of packstone, mostly with hardground (Fig. 2). The wackestone has a particle content of less than 50%, mainly benthic foraminifera, with a small amount of non-fixed bivalve and rudist clastics. This kind of rock has many bioturbated structures (Fig. 2a, 2e). This kind of rock has apparent diagenetic differences. The grayish patches are stronger cementation, but the dark parts which are surrounded the grayish patches are weaker cementation. The matrix weaker in cementation has rich micropores (Fig. 2b, 2f) and obvious oil immersion. The micrite limestone has a small number of benthic foraminifera (Fig. 2c, 2d, 2g, 2h), few pores, and most cavity pores completely cemented by calcite, and is 10–30 cm thick, accounting for less than 5%.

The hardground developed extensively, is mainly composed of micrite limestone and a small amount of wackestone. Most of the rocks have biological burrows in extension perpendicular to the bedding. The rock in the burrow is tightly cemented, and the burrows in some layers show obvious dissolution (Fig. 2c). The main body of the rock is oil-free, and only the fillings mainly composed of fine-grained debris contain micropores and have oil patches. The hardground layer is 30–50 cm thick each, accounting for about 10%.

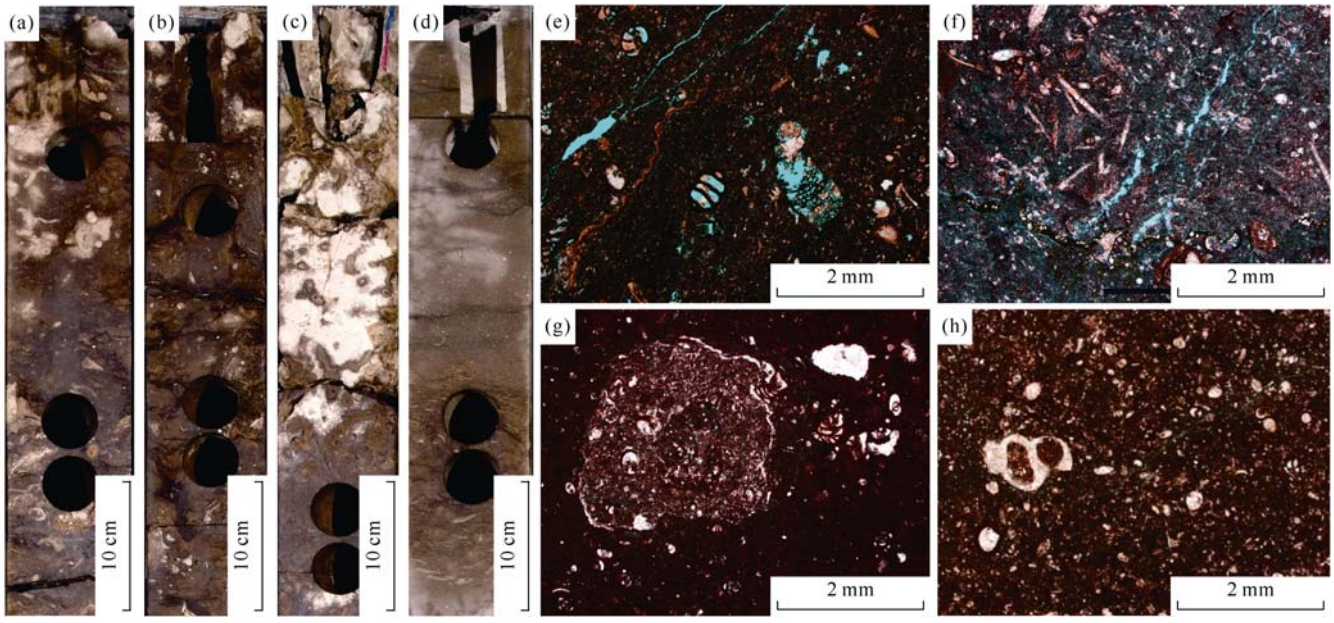

Fig. 2. Lagoon microfacies in MB1-2 sub-member of Mishrif Formation of Well M316 in Halfaya Oilfield. (a) 2935.00–2935.50 m, wackestone, with obvious bioturbation and oil patches, core photos; (b) 2918.00–2918.50 m, wackestone, with bioturbation and irregular pressure solution strip, core photos; (c) 2916.00–2916.50 m, hardground micrite-wackestone, grayish white, burrows in deep color due to oil immersion, core photo; (d) 2893.00–2893.50 m, micritie-wackestone, tight, core photo; (e) 2935.12 m, wackestone, with foraminifera and cavity pores, cast thin section; (f) 2918.16 m, wackestone, with bioclasts, and micropores in matrix, cast thin section; (g) 2916.10 m, hardground micrite-wackestone, with biological burrows filled, strongly cemented by calcite, cast thin section; (h) 2893.11 m, micrite-wackestone, with visible foraminifera microfossils and cavity completely filled with calcite, cast thin section.

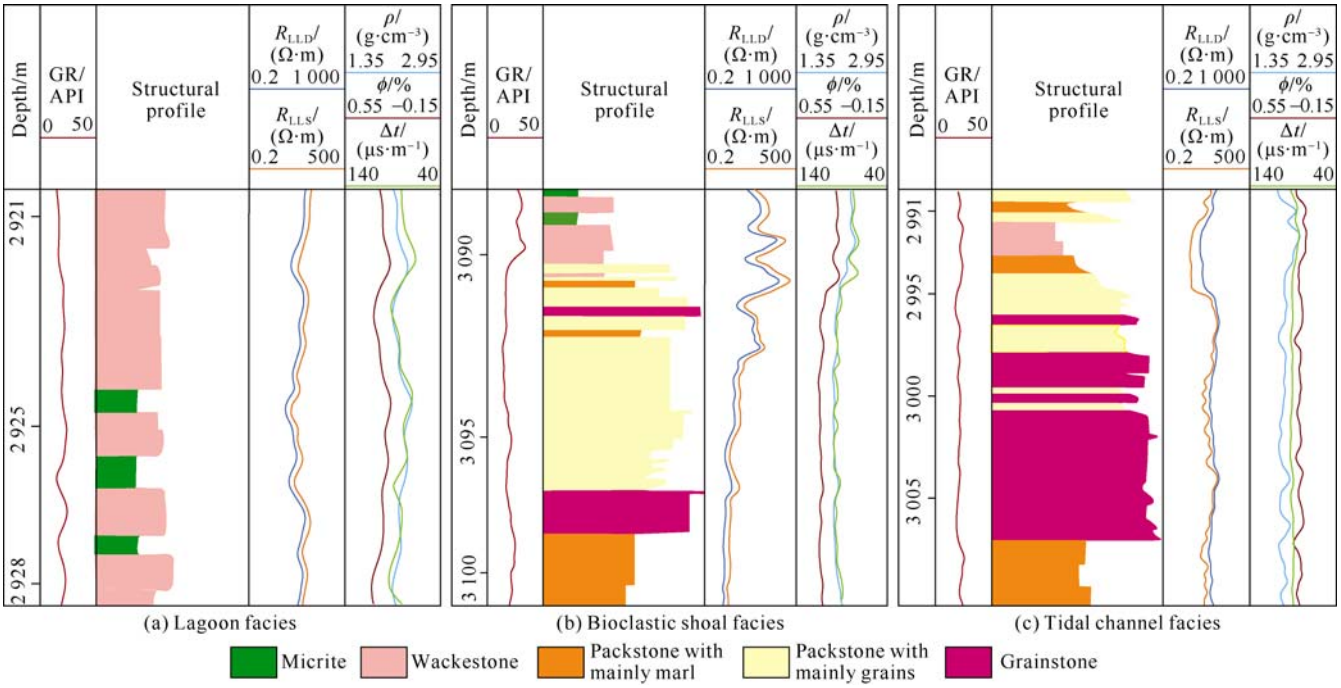

Fig. 3. Structural characteristics of various microfacies cycles in MB1-2 sub-member of Mishrif Formation in Halfaya Oilfield. GR—natural gamma; ρ—denstiy; Δt—acoustic differential time; ϕ—porosity; R_{LLD}—deep lateral resistivity; R_{LLS}—shallow lateral resistivity.

2.1.1.2. Internal structure and morphology of lagoon microfacies

The lagoon microfacies is made up of high-frequency cycles of micrite limestone–wackestone–hardground (Fig. 3a) of 1–4 m thick, mostly about 2 m thick, which is frequently separated by tight cemented hardground layers vertically. Core calibration shows that the hardground layers feature slightly low gamma value (25–28 API), high density, low neutron and acoustic time difference, while the wackestone layers feature gamma value of greater than 30 API, so the lagoon microfacies is characterized by high sawtooth fluctuations of gamma ray values (Fig. 3a). The hardground layers can extend several kilometers horizontally, forming relatively stable barriers in the lagoon microfacies.

2.1.2. Bioclastic shoal microfacies

2.1.2.1. Composition of bioclastic shoal microfacies

The bioclastic shoal microfacies contains smaller shoals in relatively high geomorphic area under the lagoon background and is mainly composed of packstones and grainstone. Medium-high energy bioclastic shoal is mainly composed of grainstone, with intergranular pores, cross beddings and changes in granularity (Fig. 4a). The medium-lower energy shoal is dominated by packstone with benthic foraminifera and non-fixed bivalve debris and a small amount of rudist and echinoderms debris, and with carbonate mud filled in the intergranular pores (Fig. 4b).

2.1.2.2. Internal structure and morphology of bioclastic shoal microfacies

The single cycle of shoal shows a reverse rhythm with the maturity of lithologic structure gradually increasing from bottom to top, i.e. the particle size increases, the mud content decreases, and the sorting becomes better. This microfacies shows low (less than 30 API) and decreasing upward values on gamma ray log, and funnel or box shape with upward increase values on resistivity log (Fig. 3b).

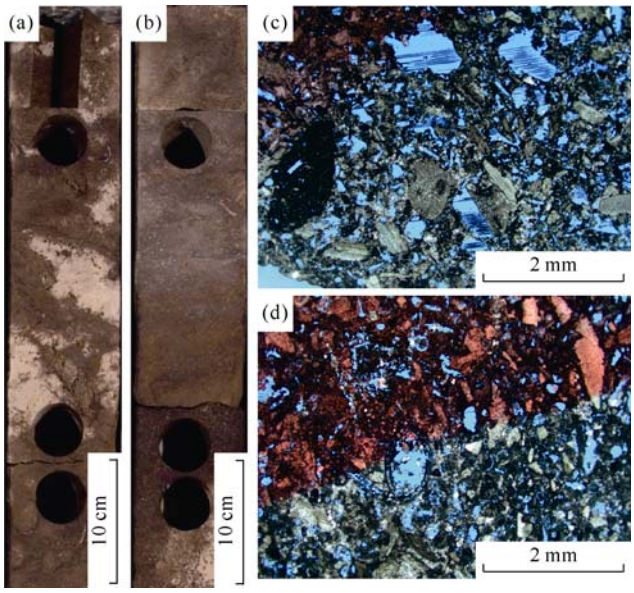

Fig. 4. Bioclastic shoal microfacies in MB1-2 sub-member of Mishrif Formation in Well N195 of Halfaya Oilfield. (a) 3061.00–3061.50 m, grainstone with cross-bedding and visible grading sequence change, core photo; (b) 3060.00–3060.50 m, packstone with obvious grain sense, core photo; (c) 3061.11 m, grainstone with intergranular pores, bioclasts of mainly non-fixed bivalves, echinoderms and spherulites, cast thin section; (d) 3060.12 m, grain dominated packstone, with intergranular pores and mold pores, and marl filling between grains, cast thin section.

Seismic impedance inversion reveals that the bioclastic

shoals are lenticular and show migration and stacking characteristics on the section; while they come in patches of irregular shape on the plane.

2.1.3. Tidal channel microfacies

2.1.3.1. Composition of tidal channel microfacies

Tidal channel sediments are mainly composed of bioclastic grainstone, packstone and wackestone. The grainstone is well sorted with visible bidirectional cross-bedding (Fig. 5a, 5e), similar to the tidal channel sediment of Feixianguan Formation in Sichuan Basin[22]. With intergranular pores well developed (Fig. 5b, 5f), the granular is saturated with oil from core observation. The packstone is grain-supported; with mainly carbonate mud filling between grains. The packstone has irregular mud-rich bands from core observation, indicating that it is still affected by current. The wackestone is rich in marl and mud bands, and contains a small amount of bioclastic and scattered euhedral dolomite formed during shallow burial.

According to the ratio of grainstone, tidal channel microfacies can be sub-divided into grain-dominated tidal channel sediment and mud-dominated tidal channel sediment.

2.1.3.2. Internal structure and morphology of tidal channel microfacies

Grain-dominated channel sediments have a typical upward-fining cycle characteristic, like the “binary structure” of fluvial sediments. The lower part is composed of grainstone, which accounts for more than half of the thickness of the tidal channel, and with increase of mud gradually upward, the upper part is mainly composed of packstone (Fig. 5c, 5g) and wackestone (Fig. 5d, 5h), which represents the cycle of development, migration and abandonment of tidal channel. The bottom of the cycle has obvious erosion. The tidal channel shows bell shape with low gamma values (less than 25API) of the lower part and gradual increase of gamma values upward. The single stage tidal channel in MB1-2 sub-member of Well Y161 can be 15 m thick (Fig. 3c).

The mud-dominated tidal channel sediments are characterized by less particle filling and mainly mud filling. Due to their similarities to lagoon microfacies in log features, these sediments are difficult to identify on cores and log curves, and need to be identified overall in combination with seismic slices.

The tidal channel microfacies can be stacked by multiple phases of tidal channel sediments. Due to the intermittent action of current and the trend of gradual weakening of water energy, tidal channel sediments have frequent migration and filling variation in space, so grainstone changes in development ratio and occurs in different positions, possibly in the lower part and edge of tidal channel, or overlapping in multiple layers; while intermittently along the tidal channel laterally.

The tide channel is similar in shape with the river channel. It shows a concave shape on the profile, and "meandering river" shape on the plane, accompanied with multi-phase migration characteristics.

2.2. Coupling of microfacies architectures

The coupling feature of microfacies architectures refer to the spatial superimposition relationship of microfacies architecture units under constraints of different levels of boundaries. It has two key elements: architecture boundary and microfacies coupling feature.

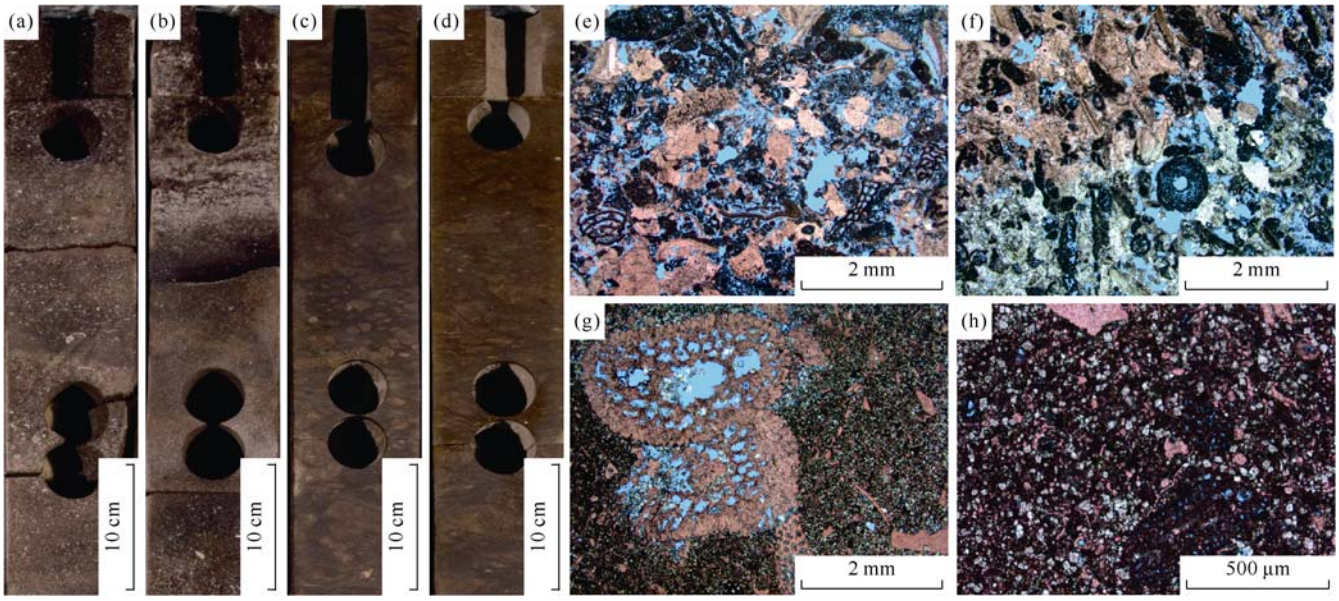

Fig. 5. Tidal channel microfacies in MB1-2 sub-member of Mishrif Formation, Well Y161 in Halfaya Oilfield. (a) 3005–3005.5 m, grainstone with bi-directional cross-bedding, core photo; (b) 3004.0–3004.5 m, grainstone, with bi-direction cross-bedding, core photo; (c) 2993.0–2993.5 m, packstone with mud-rich seams, core photo, (d) 2992.0–2992.5 m, wackestone with mud-rich seams, core photo; (e) 3005.1 m, grainstone with intergranular pores and bioclastic cavity pores, cast thin section; (f) 3004.1 m, grainstone with intergranular pores and a small number of intragranular dissolved pores, cast thin section; (g) 2993.1 m, packstone with bioclastic cavity pores, matrix micropores, and marl partially dolomitized, cast thin section; (h) 2992.1 m, wackestone with automorphic dolomite in scattered distribution, cast thin section.

2.2.1. The high frequency sequence stratigraphy and architecture boundaries

There is a complete third-order sequence in MB1-2 sub-member, and the top and bottom sequence boundaries are all type I boundaries. After the deposition of MB2 Member, the study area experienced extensive exposure and dissolution, and developed several large incised valleys as deep as 30m (Fig. 6a) in NE direction, which means that the sea level was at least 30 m below the top of the platform at that time. In the early depositional stage of MB1-2 sub-member, the incised valleys were filled with LST-TST micrite limestone, completing the level-up. In the middle-late depositional stage of MB1-2 sub-member, the oilfield area was relatively flat in terrain, and the sedimentation was mainly controlled by the rise and fall of sea level. The typical onlap above the top surface of the MB1-2A sub-layer in the western part of the study area reveals that the MB1-2A sub-layer top corresponds to a large-scale sea level fall and constitutes the top boundary of the third-order sequence. The third-order sequence boundary constrains unified sedimentary system, which is equivalent to the 8-level architecture boundary determined by Miall for clastic rocks.

The third-order sequence of MB1-2 sub-member includes three fourth-order sequences corresponding to MB1-2C, MB1-2B and MB1-2A sublayers (Fig. 6). The boundary of each fourth-order sequence can be traced on seismic section, and correlate across the oilfield. The fourth-order sequences are at a stable thickness of about 30 m each. Core observation and isotopic stratigraphic analysis show that the tops of MB1-2C and MB1-2B sublayers respectively correspond to significant sea level fall events (Fig. 6b), and have tidal channels incising into the earlier sediments, indicating during development of the tidal channels, the peripheral area was exposed to corrosion. Hence, the tops are defined as exposure and corrosion surfaces during sedimentary hiatus, roughly corresponding to the level 6 architecture boundary defined by Miall. The bottom boundary of tidal channel corresponds to level 5 architecture boundary.

The fourth-order sequences are sub-divided into nine fifth-order sequences, with top surfaces on the core appearing as secondary exposure and dissolution surfaces (Fig. 6b), which represent the top surfaces of the upward shallowing cycles, corresponding to the level 4 architecture boundary, and it is the same level as the scour surface of the single tidal channel. Below the fifth-order sequence boundary is largely bioclastic shoal, hardground or lagoon microfacies. The architecture boundaries below level 3 can be identified on the core, but cannot be characterized by logging and seismic data.

2.2.2. Coupling of microfacies architectures

The coupling analysis of microfacies architectures should be carried out in the genetic unit. The fourth-order sequences show good comparability and similarity within the area, so they are chosen for microfacies coupling analysis.

The main body of the fourth-order sequences is composed of overlapping lagoon microfacies and many micrite limestone–wackestones–hardground cycles controlled by fifth-order cycles. The lower part of the fourth-order sequence (the bottom of MB1-2C sublayer and MB1-2B sublayer) is

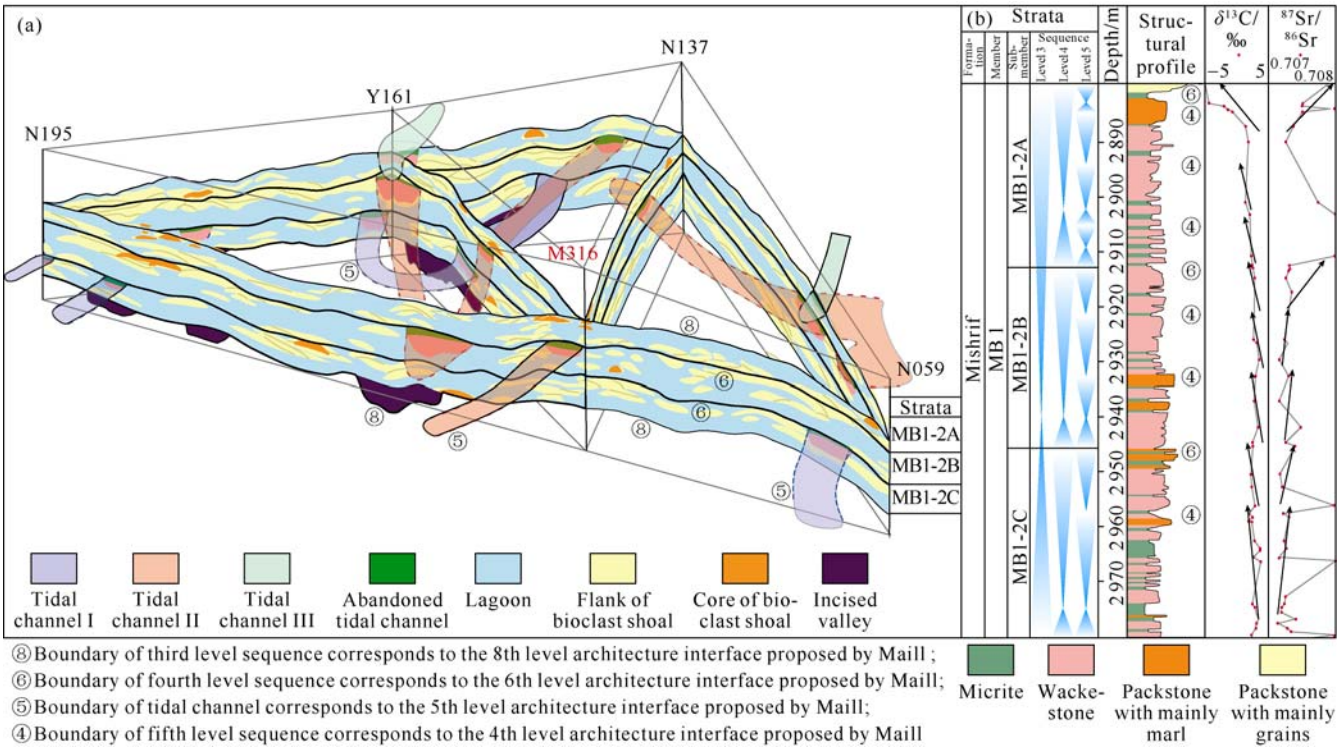

Fig. 6. Grid diagram of sedimentary architectures in MB1-2 sub-member of Mishrif Formation in Halfaya Oilfield (a) and high frequency sequence column of MB1-2 sub-member in Well M316 (b).

mainly composed of high gamma-value granular wackestones and micrites (Fig. 6b), which represents low-energy sediment during sea level rise in transgression period with good lateral comparability. The HST is dominated by wackestone–hardground cycle.

In the relatively open area or topographic relief area under the lagoon background, for example, the incised valleys were almost leveled up, but its upper edge was still characterized by slight slope, where the water energy was high, and bioclastic shoal would like to develop. Hence, wackestone–bioclastic packstone–grainstone cycle of lagoon facies developed vertically. The bioclastic shoal migrated downward to the inner side of the incised valleys and appeared as overlapping pieces in the lagoon background.

The tidal channel systems mainly occur below the fourth-order sequence boundaries, and 9 tidal channel systems in 3 phases have been identified. They are in the shape of "meandering river" on the plane, with distribution controlled by topography. The two large tidal channels developed in the MB1-2C and MB1-2B sublayers in the central east of the study area seem to be successive.

3. Reservoir architectures

Different from clastic rocks, carbonate rocks always experience epigenetic modification. Therefore, reservoir architectures of carbonate rocks are the joint effect of the microfacies architecture and diagenetic modification.

3.1. Reservoir epigenetic reformation

Previous studies and core observations in this research reveal that the interval of our interest has been reformed by various diagenetic processes, among which cementation and dissolution have strong impact on petrophysical properties and development of the reservoir.

The effect of cementation on reservoir petrophysical properties and texture is mainly manifested in the formation and development of the hardground. Thin section observation shows that the hardgrounds are mainly composed of strongly cemented micrite limestone or wackestone, so they have few pores in matrix and only some pores in fillings in the vertical burrows (Fig. 2c). The development of hardground is closely related to the frequent oscillation of sea level. The lagoon microfacies is composed of many meter-scale cycles of wackestone to hardground, which may represent the intermittent effects of hydrodynamics in a semi-restricted environment. Sea level rise would connect the open water which carried bioclastic debris in, and when the sea level fell, the water body was restricted, the sedimentation rate dropped, and then the hardground was formed.

The large-scale sea level falls at the end of the fourth-order sequences and at the end of the fifth-level sequence of TST led to dissolution (or early supergene karstification[13, 16]), and the dissolution model was similar to that proposed by Zhong et al. and Xiao et al.[16, 34–35]. The development of tidal channels at the end of the fourth-order sequence was accompanied by widely exposure of lagoons and bioclastic shoal, so the dissolution then was larger in scope and depth, resulting in the development of dissolved pores in lagoon microfacies that wasn't originally reservoir. The influence of this dissolution can go through the fifth level cycles vertically. For example, the whole upper part of MB1-2B sublayer in Well M316 is affected by the vertical dissolution, as a result, this part has a vertical permeability higher than horizontal permeability (Fig. 7), and even the vertical blocking effect of hardground in the lagoon microfacies is weakened. The identification signs of dissolution section on logging curves are: gamma value greater than 30 API, low density, and high acoustic time difference and neutron porosity (Fig. 7), which is like the features of porous lagoon microfacies.

3.2. Types and petrophysical properties of reservoir rocks

The analysis of 402 slices and porosity and permeability data shows that the sedimentary microfacies, rock types and petrophysical properties of the MB1-2 sub-member in the Halfaya Oilfield are closely correlated (Fig. 8). The reservoirs there can be divided into three types: tidal channel grainstone-packstone type, bioclastic shoal grainstone-packstone type, and lagoon wackestone dissolution modified type.

The tidal channel facies grainstone-packstone reservoirs have largely intergranular pores, with a porosity from 15.1% to 30.0% (on average 24.5%) and permeability of (1.63–200.61)×10^{-3} μm^2 (on average 72.97×10^{-3} μm^2), making class I high quality reservoir. The wackestone in the tidal channel contains mainly micropores, with a porosity of 6.85% to 32.06% (on average 18.49%), permeability of (0.03–168.55)×10^{-3} μm^2 (on average 12.80×10^{-3} μm^2), and mostly does not form effective reservoir. The bioclastic shoal facies has a porosity of 1.79%–35.35% (on average 18.29%) and permeability of (0.02–243.97)×10^{-3} μm^2 (on average 14.39×10^{-3} μm^2), of which the upper part grainstone and packstone can form high quality reservoir. The lagoon microfacies is composed of wackestone and micrite. The wackestone after dissolution has rich micropores, dissolution pores and dissolution fractures, with a porosity up to 29.06%, on average 14.99%; and a permeability up to 185.43×10^{-3} μm^2, on average 5.00×10^{-3} μm^2, can be high-quality reservoir or even high permeability layer. Although the wackestone and micrite not subjected to dissolution can have a porosity of more than 15%, they have a permeability of less than 1×10^{-3} μm^2 in general, forming barrier layers.

Different microfacies have differences in physical properties. To be specific, grainstone and packstone in tidal channel facies can form high-quality reservoirs, while the mud-dominated packstone and wackestone have relatively good porosity, but much poor permeability, and act as barriers. With a wide span of porosity and permeability, the bioclastic beach has the best reservoir in the grainstone and packstone in the core and upper part of the high-energy bioclastic shoal. The lagoon facies itself is dominated by fine-grained wackestone and micrite with small pore throat radius and low

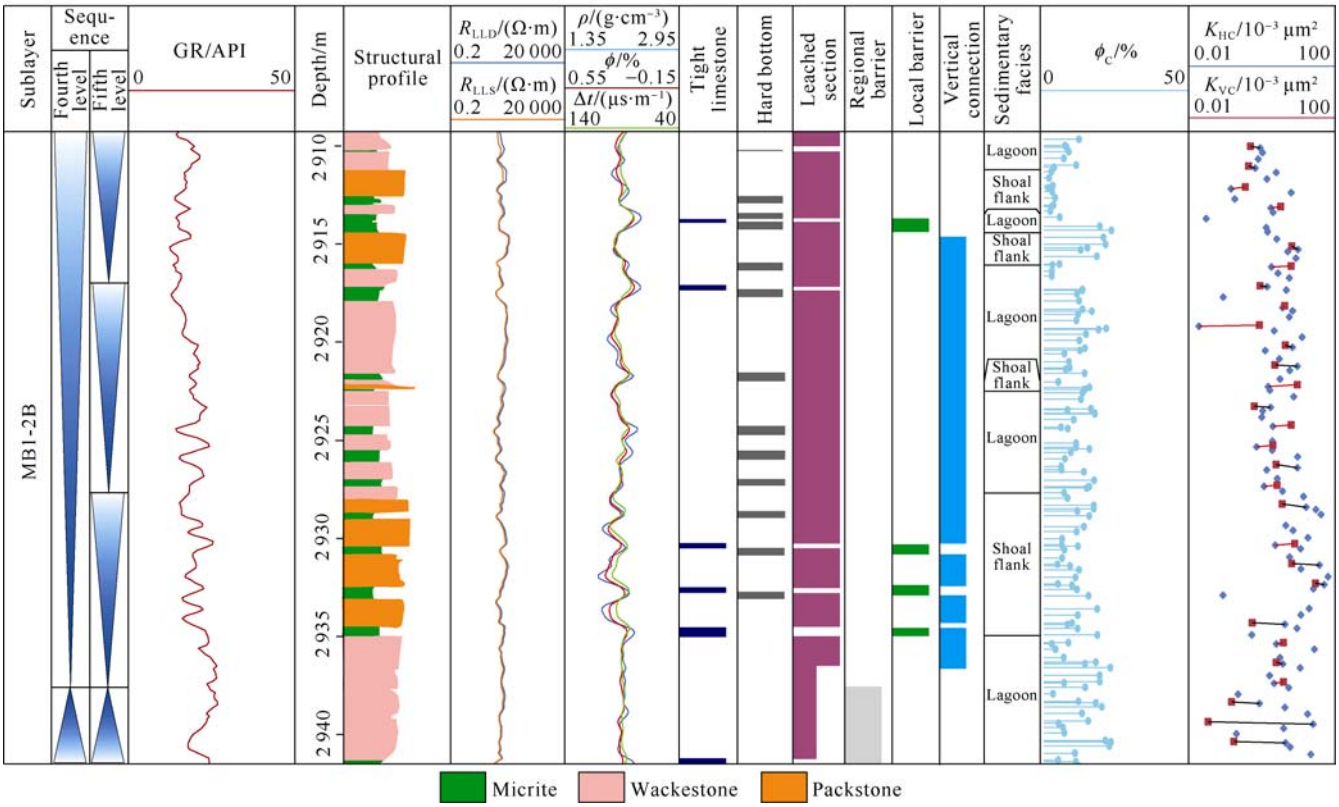

Fig. 7. Dissolution of lagoon microfacies in MB1-2 sub-member of Mishrif Formation in Halfaya Oilfield. R_{LLD}—deep lateral resistivity; R_{LLS}—shallow lateral resistivity; ρ—density; ϕ—log porosity; Δt—sonic time difference; ϕ_C—core measured porosity; K_{HC}—core measured horizontal permeability; K_{VC}—core measured vertical permeability.

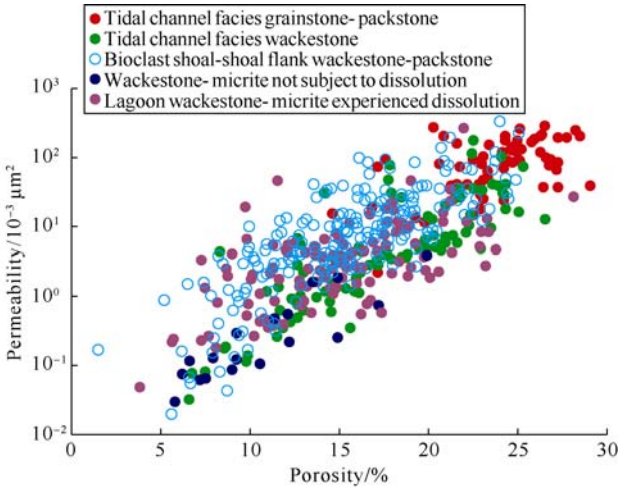

Fig. 8. Distribution of physical properties of different sedimentary formations in MB1-2 sub-member of Mishrif Formation in Halfaya Oilfield.

permeability, so it does not constitute effective reservoir, but mainly barrier layer; however, the wackestone suffered dissolution can form higher quality reservoir, and the wackestone section with rich dissolution pores and dissolution fractures can even turn out to be high permeability layer in contrast to the lagoon microfacies suffering non/weak dissolution.

3.3. Reservoir architectures

The analysis of reservoir characteristics, genesis and physical properties shows that the reservoirs in MB1-2 sub member of Mishrif Formation in the study area have the dual characteristics of facies control and diagenesis control. Under the mutual control of sedimentation architecture and sequence-controlled dissolution, the reservoirs exhibit "attic type" architecture feature in general (Fig. 9). The fourth-order sequence cycle controls the development of reservoir and the barrier layers. The dissolution associated with sequence boundaries affects the development and distribution of high permeability layers. And the high-frequency sequence cycle controls the development of barrier layers.

In lagoon microfacies poor reservoirs with different oil contents but poor permeability, there are some high-quality grainstone and packstone reservoirs of tidal channel and bioclastic shoal microfacies, as well as some dissolved lagoon facies reservoirs. Among them, the tidal channel and bioclastic shoal grainstone and packstone reservoirs are consistent in reservoir architecture and sedimentary architecture. Embedded in the lagoon microfacies background, they are typical facies-controlled reservoirs (Fig. 9). The lagoon microfacies wackestone dissolution reservoirs generally occur below fourth-order sequence boundaries, and the high-quality reservoirs come in layers with big variations in thickness. The dissolution intensity may be controlled by parent rock composition and micro-landform (Fig. 9). The dissolution may connect the bioclastic shoal reservoir with lagoon reservoir, enlarging the reservoir scale.

The lagoon microfacies wackestone and micritic limestone

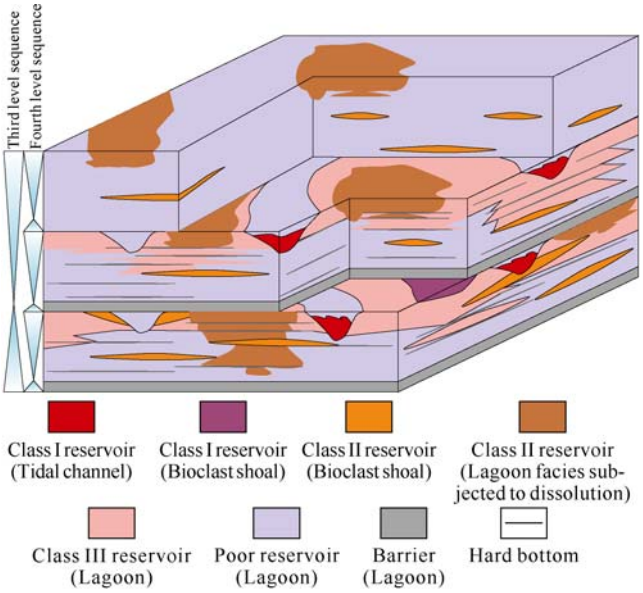

Fig. 9. Microfacies architectures (a) and reservoir architectures (b) of MB1-2 sub-member in Mishrif Formation, Halfaya Oilfield.

deposited in transgression periods not subjected to dissolution with poor physical properties, a thickness of about 10 m and stable distribution, can form good regional barrier layers separating reservoirs in HST.

None or slightly dissolved wackestone and hardground sections form barrier layers inside the reservoir. Although the hardground section is less than 0.5 m thick, it can extend for tens of kilometers and significantly affect the fluid flow. At the same time, due to the influence of extensive dissolution in local parts, the biological burrows after dissolution may make originally separated reservoirs connect with each other (Fig. 9).

Because of migration and multi-stage waterflow reconstruction on the tidal channel facies, there are usually many sets of grainstone sandwiched between wackestone layers inside the tidal channel, leading to complex reservoir architectures. At the same time, due to the difference of microfacies incised by tidal channel (Fig. 9), the reservoirs vary greatly in architecture, for example, if tidal channel incises lagoon facies, the grainstone in the tidal channel would form reservoir independently; if tidal channel incises the bioclastic shoal facies, the grainstone filling the tidal channel may piece together with the bioclastic shoal grainstone to form a composite reservoir. If the tidal channel is mainly filled with wackestone, then it may act as a barrier to the reservoir (Fig. 9).

4. Implications to reservoirs development

The analysis of sedimentary and reservoir architectures reveals that the oil reservoir of the MB1-2 sub-member in Mishrif Formation has strong heterogeneity, vertically separated by different sizes of barriers or interlayers, and complicated microfacies and reservoir architectures laterally, which will inevitably affect the fluid percolation features and reservoir development mode. The influence mainly reflects in following three aspects.

4.1. Separated layer water injection according to interlayer development pattern

Examining the production data before, it is found that barriers with a permeability of less than 3×10^{-3} μm^2 can effectively isolate reservoirs. The analysis of rock types and physical property data shows that the rocks can act as barriers in the MB1-2 sub-member of the study area are micritic limestone and wackestone of lagoon facies haven't subjected to dissolution which have permeability 1-2 orders lower than packstone and grainstone reservoirs. Vertical sequence analysis shows that barrier layers mainly occur in the lower part of the TST of the fourth-order sequences, especially barrier of micritic limestone and wackestone at the bottom of the MB1-2C sub-layer with stable thickness and continuous distribution in the region works as a regional barrier, dividing MB2 Member and MB1 Member into two oil pools. Wackestone layer at the bottom of the MB1-2B sub-layer is relatively stable in most areas, separating MB1-2B sub-member from MB1-2C sub-member (Fig. 9).

In the early stage, Mishrif Formation in Halfaya Oilfield was developed by depletion. With the increase of production wells, the reservoir pressure and well production have dropped, and the oilfield is gradually turning to water injection development. As there are relatively stable barriers and large physical property differences between reservoirs in MB1 Member, separated layer water injection is the premise to ensure good effect of water injection development[36]. The MB1-2C sub-layer of Mishrif Formation has a relatively stable barrier at its top, so the one set injection-production well pattern for MB1 reservoir is changed to two sets injection-production well patterns.

Considering the frequent alternating thin layers of lagoon facies and the local blocking effect of the hardgrounds, how to improve the sweep efficiency will become the key concern.

4.2. Well pattern design and well trajectory optimization according to microfacies coupling features

The strong spatial heterogeneity of the reservoir in MB1-2 sub-member of Mishrif Formation makes irregular well pattern more suitable for the reservoir. Regular well pattern can be adopted for dissolved lagoon wackestone reservoirs and bioclastic shoal grain limestone-packstone reservoirs. Because the dissolution near the fourth-order sequence boundary is likely to connect these two kinds of reservoirs into a larger reservoir unit. However, for the tidal channel grainstone to packstone reservoir, if it incises lagoon facies with poor physical properties, they are often spatially independent, and the regular well pattern cannot control the direction of tidal channel reservoir. Even if the tidal channel incises bioclastic shoal or porous lagoon facies to form a unified reservoir unit, their different pore structures may result in complicated internal percolation features, and regular well pattern would lead to

to complicated distribution of remaining oil. Therefore, it is necessary to set up oil wells and water wells according to the architecture of tidal channel. In view of complex reservoir architectures, in the design of well trajectory, we should try to improve the reservoir drilling rate and single well utilization.

4.3. Optimization of water injection strategy according to the development of high permeability layers

Through the analysis of reservoir architectures, there are two types of high permeability layers, i.e. sedimentary-type and diagenetic-type, in the upper member of the Mishrif Formation in the study area, which have different development patterns and different effects on water injection strategy.

The sedimentary-type high permeability layers have abnormally higher permeability than lagoon facies reservoirs due to different rock types, they are mostly tidal channel and bioclastic shoal grainstone layers with permeability 1–2 orders of magnitude higher than the lagoon facies packstone or wackestone layers, making them high permeability channels. Although the lagoon facies wackestone with a porosity of more than 10%, can be effective reservoir, the high permeability grainstone layer will inevitably prohibit the fluid flowing into the lagoon facies layer during oil and gas exploitation or water injection. Without understanding on the tidal channel architecture, this prohibition effect could be misinterpreted as the effect of high permeability layer. Due to the particularity of tidal channel architecture, a separate injection-production system should be established for the tidal channel.

The diagenetic-type high permeability layer is mainly formed by the exposure dissolution associated with the tidal channel development at the end of the fourth-order sequence. Partially dissolved wackestone with rich dissolved pores can have abnormally high permeability, and make high permeability layer, i.e. diagenetic-type high permeability layer. This kind of high permeability layer has been confirmed in the well group M325. The development of this type of high permeability layer is controlled by the sequence boundary, so the water injection interval chosen shouldn't be too close to the sequence boundary, to avoid fast advancing of injected water and swept volume reduction caused thereof.

In addition, the exposure dissolution may cause separation failure of some hardground layers, and the vertical connectivity is also a concern in the analysis of the effectiveness of water injection.

5. Conclusions

The MB1-2 sub-member of Mishrif Formation is mainly composed of packstone or wackestone, and consists of lagoon facies, bioclastic shoal facies and tidal channel facies. Lagoon facies is made up of micrite limestone–wackestone–hardground cycles. The bioclastic shoals appear in pieces on the background of lagoon. Tidal channel system mainly occurs below the fourth-order sequence boundary, and takes on "meandering rive" shape on the plane.

Reservoir architectures are controlled by both sedimentary facies and diagenesis. Tidal channel and bioclastic shoal grainstone and packstone layers can be high quality reservoirs, and have high permeability layers of sedimentation type. The lagoon facies mainly constitute barrier layers. Lagoon facies wackestone layer experienced dissolution can be good reservoir and diagenetic-type high permeability layer.

The reservoirs in the MB1-2 sub-member of Mishrif Formation overlap in "attic" pattern, and there are relatively stable barriers between the reservoir sections, therefore, it is suitable to be developed by separated layer water injection. According to the sedimentary architectures, irregular well pattern and well trajectory should be adopted to improve the drilling rate of the reservoir. The water injection strategy should be optimized according to the type and distribution of high permeability layers to improve the development effectiveness.

References

[1] EHRENBERG S N, AQRAWI A A, NADEAU P H. An overview of reservoir quality in producing Cretaceous strata of the Middle East. Petroleum Geoscience, 2008, 14: 307–318.

[2] AQRAWI A A. Paleozoic stratigraphy and petroleum systems of the western and southwestern deserts of Iraq. GeoArabia, 1998, 3: 229–248.

[3] ALSHARHAN A S, NAIRN A E. A review of the Cretaceous formations in the Arabian Peninsula and Gulf: Mid Cretaceous stratigraphy and paleogeography. Journal of Petroleum Geology, 1988, 11: 89–112.

[4] MAHDI T A, AQRAWI A A. Sequence stratigraphic analysis of the mid Cretaceous Mishrif Formation, southern Mesopotamian Basin, Iraq. Journal of Petroleum Geology, 2014, 37: 287–312.

[5] SADOONI F N. The nature and origin of Upper Cretaceous basin margin rudist buildups of the Mesopotamian Basin, southern Iraq, with consideration of possible hydrocarbon stratigraphic entrapment. Cretaceous Research, 2005, 26: 213–224.

[6] GAO Jixian, TIAN Changbing, ZHANG Weimin, et al. Characteristics and genesis of carbonate reservoir of the Mishrif Formation in the Rumaila oil field, Iraq. Acta Petrolei Sinica, 2013, 34(5): 843–852.

[7] TIAN Zepu, LIU Bo, GAO Jixian. Diagenesis of bioclastic carbonates of the Cretaceous Mishrif Formation in the Rumaila oil field, Iraq. Journal of Stratigraphy, 2016, 40(1): 41–50.

[8] ZHOU Wen, GUO Rui, FU Meiyan, et al. Characteristics and origin of Cretaceous limestone reservoir with bio-moldic pore and ntrafossil pore, in Ahdeb oilfield, Iraq. Acta Petrologica Sinica, 2014, 30(3): 813–821.

[9] WANG Jun, GUO Rui, ZHAO Limin, et al. Geological features of grain bank reservoirs and the main controlling factors: A case study on Cretaceous Mishrif Formation, Halfaya Oil-

field, Iraq. Petroleum Exploration and Development, 2016, 43(3): 367–377.

[10] DENG Hucheng, ZHOU Wen, GUO Rui, et al. Pore structure characteristics and control factors of carbonate reservoirs: The middle-lower Cretaceous formation, AI Hardy cloth Oilfield, Iraq. Acta Petrologica Sinica, 2014, 30(3): 801–812.

[11] HAN Haiying, MU Longxin, GUO Rui, et al. Characteristics and controlling factors of Cretaceous bioclastic limestone reservoirs in Ahdeb oil field, Iraq. Marine Origin Petroleum Geology, 2014, 19(2): 54–63.

[12] YU Yichang, SUN Longde, SONG Xinmin, et al. Sedimentary diagenesis of rudist shoal and its control on reservoirs: A case study of Cretaceous Mishrif Formation, H Oilfield, Iraq. Petroleum Exploration and Development, 2018, 45(6): 1007–1019.

[13] ZHAO Limin, ZHOU Wen, ZHONG Yuan, et al. Control factors of reservoir oil-bearing difference of Cretaceous Mishrif Formation in the H oilfield, Iraq. Petroleum Exploration and Development, 2019, 46(2): 302–311.

[14] ZHANG Yikai, KANG An, MIN Xiaogang, et al. Characteristics and genesis of carbonate reservoirs in the Mishrif MB12 member in the Missan oil fields, Iraq. Petroleum Geology and Experiment, 2016, 38(3): 360–365.

[15] FU Meiyan, ZHAO Limin, DUAN Tianxiang, et al. Reservoir and early diagenesis characteristics of rudist shoal of Mishrif Formation in HF oil field of Iraq. Journal of China University of Petroleum (Edition of Natural Science), 2016, 40(5): 1–9.

[16] ZHONG Y, TAN X C, ZHAO L M, et al. Identification of facies-controlled eogenetic karstification in the Upper Cretaceous of the Halfaya Oilfield and its impact on reservoir capacity. Geological Journal, 2019, 54: 450–465.

[17] ZHONG Y, ZHOU L, TAN X C, et al. Characteristics of depositional environment and evolution of Upper Cretaceous Mishrif Formation, Halfaya Oil field, Iraq based on sedimentary microfacies analysis. Journal of African Earth Sciences, 2018, 140: 151–168.

[18] MIALL A D. Architectural-element analysis: A new method of facies analysis applied to fluvial deposits. Earth Science Reviews, 1985, 22: 261–308.

[19] WU Shenghe. Reservoir characterization and modeling. Beijing: Petroleum Industry Press, 2010.

[20] WU Shenghe, ZHAI Rui, LI Yupeng. Subsurface reservoir architecture characterization: Current status and prospects. Earth Science Frontiers, 2012, 19(2): 15–23.

[21] ZHU Weihong, WU Shenghe, YIN Zhijun, et al. Braided river delta outcrop architecture: A case study of Triassic Huangshanjie Formation in Kuche Depression, Tarim Basin, NW China. Petroleum Exploration and Development, 2016, 43(3): 482–489.

[22] QIAO Z F, JANSON X, SHEN A J, et al. Lithofacies, architecture, and reservoir heterogeneity of tidal-dominated platform marginal oolitic shoal: An analogue of oolitic reservoirs of Lower Triassic Feixianguan Formation, Sichuan Basin, SW China. Marine and Petroleum Geology, 2016, 76: 290–309.

[23] QIAO Z F, SHEN A J, ZHENG J F, et al. Digitized outcrop geomodeling of Ramp Shoals and its reservoirs: As an example of Lower Triassic Feixianguan Formation of eastern Sichuan Basin. Acta Geologica Sinica (English Edition), 2017, 91(4): 1395–1412.

[24] QIAO Zhanfeng, SHEN Anjiang, ZHENG Jianfeng, et al. Three-dimensional carbonate reservoir geomodeling based on the digital outcrop model. Petroleum Exploration and Development, 2015, 42(3): 328–337.

[25] AQRAWI A A, GOFF C, HORBURY A D, et al. The petroleum geology of Iraq. Bucks: Scientific Press, 2010.

[26] Al-QAYIM B. Sequence stratigraphy and reservoir characteristics of the Turonian–Coniacian khasib formation in central Iraq. Journal of Petroleum Geology, 2010, 33: 387–403.

[27] BUDAT T, JASSIM S Z. The regional geology of Iraq. Baghdad: Publication of the Geological Survey of Iraq, 1987.

[28] DUNNINGTON H V. Generation, migration, accumulation, and dissipation of oil in Northern Iraq. GeoArabia, 2005, 10(2): 39–84.

[29] OWEN R M, NAER S N. Stratigraphy of the Kuwait Basrah area: WEEKS L G. SP18: Habitat of oil. Tulsa: AAPG, 1958: 1252–1278.

[30] ALSHARHAN A S. Facies variation, diagenesis and exploration potential of Cretaceous rudist-bearing carbonate of the Arabian Gulf. AAPG Bulletin, 1995, 79(4): 531–550.

[31] CHAMPAGNE J, DURLET C, GRéLAUD C, et al. Unconformities in the Cenomanian Turonian carbonate platform of the Middle East: Diagenetic patterns and impact on reservoir properties examples from Mishrif and Natih Formations. Revue Roumaine de Chimie, 2012, 57: 85–93.

[32] MAHDI T A, AQRAWI A A, HORBURY A D, et al. Sedimentological characterization of the mid-Cretaceous Mishrif reservoir in southern Mesopotamian Basin, Iraq. Geoarabia, 2013, 18(1): 139–174.

[33] MAHDI T A, AQRAWI A A. Sequence stratigraphic analysis of the mid-Cretaceous Mishrif Formation, southern Mesopotamian Basin, Iraq. Journal of Petroleum Geology, 2014, 37(3): 287–312.

[34] XIAO D, ZHANG B J, TAN X C, et al. Discovery of a shoal-controlled karst dolomite reservoir in the Middle Permian Qixia Formation, northwestern Sichuan Basin, Southwest China. Energy Exploration & Exploitation, 2018, 36(4): 686–704.

[35] XIAO D, TAN X C, XI A H, et al. An inland facies-controlled eogenetic karst of the carbonate reservoir in the Middle Permian Maokou Formation, southern Sichuan Basin, SW China. Marine and Petroleum Geology, 2016, 72: 218–233.

[36] SONG Xinmin, LI Yong. Optimum development options and strategies for water injection development of carbonate reservoirs in the Middle East. Petroleum Exploration and Development, 2018, 45(4): 679–689.